

## Seasonality of isotopic and chemical composition of snowpack in the vicinity of Jang Bogo Station, East Antarctica

Soon Do Hur<sup>1</sup>, Jiwoong Chung<sup>1</sup>, Yalalt Namgerel<sup>1,2</sup> and Jeonghoon Lee<sup>2,\*</sup>

<sup>1</sup>Division of Glacial Environmental Research, Korea Polar Research Institute, 26,  
Songdomirae-ro, Yeonsu-gu, Incheon 21990, Korea

<sdhur@kopri.re.kr> <jjw79@kopri.re.kr>

<sup>2</sup>Department of Science Education, Ewha Womans University, 52, Ewhayeodae-gil,  
Seodaemun-gu, Seoul 120-750, Korea

<yalaltn@gmail.com> <jeonghoon.d.lee@gmail.com>

\* corresponding author

**Abstract:** Seasonal variations of the isotopic and chemical compositions of snowpits can provide useful tools for dating the age of the snowpit and examining the sources of aerosol. Based on the seasonal layers with  $\delta D$  and  $\delta^{18}O$  maxima and minima, it was determined that the snowpit, conducted in the vicinity of the Jang Bogo Station in Antarctica, contained snow deposited over a three-year period (2008–2010). Distinct seasonal variations of stable water isotopes were observed, with a slope of 8.2 from the linear isotopic relationship between oxygen and hydrogen, which indicates that the snow accumulated during three years without a significant post-depositional process. The positive correlations ( $r > 0.85$ ) between  $Na^+$  and other ions in the winter period and the positive relationship the concentrations of the methanesulphonic acid (MSA) and non-sea salt sulfate ( $nssSO_4^{2-}$ ) in the warm period ( $r = 0.6$ , spring to summer) indicate the significant contributions of an oceanic source to the snowpit. Based on principal component analysis, the isotopic and chemical variables were classified

into species representing input of sea-salt aerosol and suggesting potential seasonal markers. This study will support further investigations using ice cores in this region.

**Keywords:** Antarctica, Terra Nova Bay, snowpit, water stable isotopes, snow chemistry.

## Introduction

Information on the spatial and temporal variabilities of snow chemistry is crucial in glaciochemical studies (Dansgaard 1964; Jouzel and Masson-Delmotte 2010). Snowpit and ice cores provide robust records of the past climate and environmental changes, particularly in remote areas such as Antarctica where instrumental data are sparse and have short observation periods (Jouzel *et al.* 2007; Sinclair *et al.* 2010; Klein *et al.* 2019). In Antarctica, many of the chemical species and isotopic compositions of water retrieved from ice cores and snowpits show clear seasonal variations (Kuramoto *et al.* 2011; Kwak *et al.* 2015; Nyamgerel *et al.*, 2020, 2021). Distinguishing seasonal patterns in stable water isotopes ( $\delta^{18}\text{O}$  and  $\delta\text{D}$ ) and chemical impurities is crucial for the stratigraphic dating of accumulated snow layers, and are used as proxies for temperature, sea ice extent, atmospheric circulation, and aerosol transport and depositional processes (Udisti 1996; Delmotte *et al.* 2000; Ayling and McGowan 2006; Severi *et al.* 2017; Du *et al.* 2019; Servettaz *et al.* 2020). However, obtaining reliable relationships between chemical and isotopic data and atmospheric composition is strongly dependent on how changes in source intensity and transport efficiency can be stored in snow in different climatic conditions (Udisti *et al.* 1999; Stenni *et al.* 2000; Rhodes *et al.* 2012; Markle *et al.* 2012; Tuohy *et al.* 2015; Arndt *et al.* 2018; Casado *et al.* 2018; Goursaud *et al.* 2018; Ma *et al.* 2020; Servettaz *et al.* 2020).

In 1988, the Republic of Korea constructed its first permanent year-round base in Antarctica, named King Sejong Station ( $62^{\circ} 13.4'S$ ,  $58^{\circ} 47.3'W$ ), on King George Island,

South Shetlands. However, given its distance from the Antarctic continent, the extent of in-depth research and international collaboration around the King Sejong Station has been limited. In this context, the construction of a second Korean scientific research station in Antarctica was proposed in 2004; this station was completed in 2014 and named the Jang Bogo Science Station (JBS). Its location is appropriate for conducting studies on the reconstruction of past climate and environment using ice cores, geological surveys, and so on (Park *et al.* 2014). The station is located in mainland Antarctica on the coast of Terra Nova Bay (TNB), northern Victoria Land ( $74^{\circ} 37.4'S$ ,  $164^{\circ} 13.7'E$ ; Fig. 1). In TNB, there is also an Italian summer research station, the Mario Zucchelli Station, which is located at a distance of  $\sim 10$  km to the southwest of the JBS. The latitude of the JBS is nearly  $10^{\circ}$  higher than that of the King Sejong Station on King George Island and the climate is close to that of Antarctica (Park *et al.* 2014). The mean temperature at the JBS is  $-14^{\circ}\text{C}$  and the minimum temperature is  $-36^{\circ}\text{C}$ . Low-pressure systems are common in this region due to the influence of the Ross Sea and Transantarctic Mountains. Typically, summer is characterized by light winds, intersperse by katabatic drainage events. Westerly winds dominated and daily mean wind speeds range from  $0.5$  to  $38.6 \text{ m s}^{-1}$  (Wang *et al.* 2017).

During the 2010/2011 Antarctic expedition by the Korea Polar Research Institute (KOPRI), samples were taken from a snowpit with a depth of  $1.95$  m located  $23$  km to the north of the JBS. We selected the sampling site considering the proximity to the Styx Glacier for ice core drilling and the automatic weather systems maintained by the Mario Zucchelli Station. The Styx Glacier plateau has been characterized by high snow accumulation rates and has been of great importance in interpreting climatic and environmental change as it allows reliable dating of ice cores and the possibility to compare firn core stratigraphy with reliable satellite data, *e.g.*, sea ice extent (Nyamgerel *et al.* 2020).

Site-based information and the evaluation of seasonal variations in isotopic and

chemical compositions of snow are required to examine the present-day snow compositions and their differences at regional and/or local scales, which provide reference for the interpretation of the paleoclimate records from this region (Stenni *et al.* 2000; Tuohy *et al.* 2015; Stenni *et al.* 2017; Goursaud *et al.* 2019). To assist in ice-core interpretation at the Styx Glacier in northern Victoria Land, the purpose of this study is to evaluate the isotopic and chemical compositions of the snowpit and to determine the factors that had the greatest influence on these compositions.

## Material and methods

**Site location and sampling.** – The sampling areas in northern Victoria Land, East Antarctica, are located to the west of the coast of the Ross Sea and 23 km north of the JBS (Fig. 1). Samplings were carried out between 03 and 14 February 2011, before the construction of the JBS. Two types of samples were collected: surface snow and snowpit. Four surface snow samples were collected near the JBS to allow a comparison with the snowpit samples from the 1.95-m-deep snowpit (Table 1). The wall of the pit was removed using pre-cleaned light-density polyethylene (LDPE) shovels. Samples were obtained at depth intervals of 0.05 m with a pre-cleaned polytetrafluoroethylene (PTFE) tube and a hammer and were then transferred into pre-cleaned 1L LDPE bottles. The snowpit samples were shipped and stored frozen before isotopic and chemical analysis at the KOPRI. The samples were melted at room temperature in a clean room before being subsampled and filtered using a 0.45- $\mu\text{m}$  polyvinylidene difluoride syringe filter (Merck Millipore, USA).

**Isotopic and chemical analysis.** – A total of 39 samples were analyzed for isotopic composition by cavity ring-down spectroscopy (L1102-i, L2130-i; Picarro Inc., USA). The D/H and  $^{18}\text{O}/^{16}\text{O}$  ratios are expressed in the  $\delta$  notation as parts per thousand difference relative to the Vienna Standard Mean Ocean Water (VSMOW). The VSMOW (0‰ for  $\delta^{18}\text{O}$

and  $\delta D$ ), Greenland Ice Sheet Precipitation ( $-24.76\%$  for  $\delta^{18}O$  and  $-189.5\%$  for  $\delta D$ ), and Standard Light Antarctic Precipitation ( $-55.5\%$  for  $\delta^{18}O$  and  $-428\%$  for  $\delta D$ ) from the International Atomic Energy Agency were used to calibrate the isotopic analysis. An in-house reference prepared from Antarctic snowmelt ( $-34.6 \pm 0.07\%$  for  $\delta^{18}O$  and  $-272.4 \pm 0.6\%$  for  $\delta D$ ) was measured every 10 samples to monitor the operation of the analyzer. The analytical reproducibility was  $< 0.1\%$  and  $< 1\%$  for  $\delta^{18}O$  and  $\delta D$ , respectively. The deuterium excess ( $d$ -excess,  $\delta D = 8 \times \delta^{18}O - 10$ ), which represents the deviation from the global meteoric water line (GMWL), was estimated using the method of Dansgaard (1964).

Ions ( $Na^+$ ,  $K^+$ ,  $Ca^{2+}$ ,  $Mg^{2+}$ ,  $Cl^-$ ,  $SO_4^{2-}$  and  $NO_3^-$ ) and methanesulphonic acid (MSA) were analyzed using a two-channel ion chromatography system (ICS-200 and ICS-2100; Thermo Fisher Scientific Inc., USA) at the KOPRI. Anions were analyzed using a Dionex model ICS-2000 with an IonPac AS15 column and KOH eluent (6–55 mM), and cations were measured using a Dionex model ICS-2100 with an IonPac CS12A column and MSA eluent (20 mM). The analytical detection limit, reproducibility, and accuracy were, respectively, 0.01–0.26  $\mu g/l$ , 0.4–17.4%, and 4.5–12.0% for cations and 0.02–0.26  $\mu g/l$ , 0.1–27.6%, and 1.3–5.6% for anions. Using the theoretical ratio of a specific ion to  $Na^+$  in sea water, the non-sea-salt (nss) fraction of the sulfate was estimated to isolate the contribution of sea-spray using the following equation, assuming that  $Na^+$  was exclusively of sea-salt origin (Kuramoto *et al.* 2011):

$$[nssCl^-] = [Cl^-] - (Cl^-/Na^+)_{sea} \times Na^+ \quad (1)$$

where  $(Cl^-/Na^+)_{sea}$  is the equivalent concentration ratio of  $Cl^-/Na^+$  in the sea water, which is 1.16. Similarly, the concentration of  $nssSO_4^{2-}$  was calculated using a sea-water ratio of 0.12 (Pilson 2013).

**Principal component analysis.** – Principal component analysis (PCA), a multivariate statistical technique, is applicable to classify large datasets (Lee *et al.* 2008). PCA reduces the

information in many variables into a set of weighted linear combinations of those variables, which does not differentiate between common and unique variance. Since PCA is based entirely on the eigenvalue analysis of a correlation or covariance matrix, the data are not required to be normally distributed (Ko *et al.* 2010). In this work, PCA was applied to a correlation matrix because the variables considered in this study vary by different orders of magnitude. PCA has been used to analyze hydrochemical data, including isotopic and chemical compositions. Several studies have applied PCA to measure proxies for past atmospheric conditions from ice core records (Knüsel *et al.* 2005) and snow pits (Kwak *et al.* 2015). In this work, PCA was applied to the correlation matrix using the JMP® statistical software. Values for elements below the detection limit (DL) were substituted with DL/2 prior to statistical treatment (Lee *et al.* 2008).

## Results and interpretation

The isotopic and chemical compositions of four surface snow samples (JBG-01, JBG-02, JBG-03, JBG-04) and snowpit collected near the JBS are summarized in Table 1. The stable water isotopes ( $\delta^{18}\text{O}$ ) of the surface snow samples show similar values ( $-13.88$  to  $-18.15\text{‰}$ ) to the maximum value of the snowpit ( $-16.37\text{‰}$ ). Moreover, a slight decrease in  $\delta^{18}\text{O}$  of  $2.88\text{‰}$  was observed corresponding to the distance  $\sim 1.6$  km between JBG-01 and JBG-04 (the nearest site to the coast). The chemical compositions of the surface snow were higher than those of the snowpit. Because of the proximity of the four surface snow samples to the ocean, their isotopic and chemical compositions indicated that the source of snow was oceanic (*e.g.* Benassai *et al.* 2005; Ma *et al.* 2020). Compared to the surface snow samples JBG-02, JBG-03, and JBG-04, sample JBG-01, which was obtained farthest from the coast, showed much lower chemical compositions and more enriched isotopic values with higher *d*-excess. In the following, the isotopic and chemical compositions of the snowpit will be

presented and discussed.

**Seasonal pattern of stable water isotopes.** – In the snowpit, we observed thin ice layers with a thickness of approximately 5 mm or less at depths of 100 and 180 cm, which were formed by minor surface snowmelt during the summer months. Significant melt can alter the natural layering of snow (Udisti *et al.* 1998; Lee *et al.* 2014, 2020). However, the occurrences of slight summer surface melting apparently did not affect the profiles of stable water isotopes and ions since the isotopic compositions showed regular variations (Fig. 2). The slope of the  $\delta\text{D}$ – $\delta^{18}\text{O}$  diagram for the snowpack is  $8.2 (\pm 0.2)$ , which is close to the slope of the Global Meteoric Water Line (slope = 8; Dansgaard 1964) and the whole Antarctic scale (Local Meteoric Water Line, LMWL, slope = 7.75; Masson-Delmotte *et al.* 2008), suggesting that the vapor source came from the nearby ocean by evaporation (Uemura *et al.* 2008). This may reflect the minimal effects of sublimation and melting (Steen-Larsen *et al.* 2014; Lee *et al.* 2010; Casado *et al.* 2018). Examining the slope of the  $\delta^{18}\text{O}$  vs.  $\delta\text{D}$  regression line may reveal whether water has experienced significant evaporation, isotopic exchange between liquid water and ice, or transport from the ocean (Lee *et al.* 2009; Lee *et al.* 2010). The linear  $\delta^{18}\text{O}$ – $\delta\text{D}$  diagram for the snowpit samples is shown in Fig. 2. Physical processes such as evaporation, isotopic exchange between liquid water and ice, or isotopic exchange between water vapor and ice affect the slope of the isotopic regression line, which is typically  $< 8$  (Lee *et al.* 2009, 2010; Ham *et al.* 2019).

The stable water isotopic compositions of snowpits, firn cores, and ice cores can be used to date these deposits. Figure 3 shows the vertical profiles of the stable water isotopes ( $\delta^{18}\text{O}$ ) and deuterium excess (*d*-excess,  $d = \delta\text{D} - 8 \times \delta^{18}\text{O}$ ) sampled from the snowpit. The  $\delta^{18}\text{O}$  values ( $n = 39$ ) fluctuated between  $-35.45\text{‰}$  and  $-16.37\text{‰}$  ( $-24.34 \pm 4.84\text{‰}$ , average  $\pm 1\sigma$ ), while the  $\delta\text{D}$  values ( $n = 39$ ) fluctuated between  $-279.56\text{‰}$  and  $-125.82\text{‰}$  ( $-186.50 \pm 39.82\text{‰}$ ), which is more enriched than previous reports from the Styx Glacier (Stenni *et al.* 1999, 2000;

Kwak *et al.* 2015; Nyamgerel *et al.* 2020). This enrichment can be attributed to the snowpit's proximity to the ocean. The means of isotopic composition of oxygen from the snowpit was more enriched in heavier isotopes ( $-25.3 \pm 4.8\text{‰}$ ) relative to the previous studies reporting mean values of  $-36.2 \pm 5.0\text{‰}$  (Nyamgerel *et al.* 2021) and  $-32.9 \pm 3.2\text{‰}$  (Stenni *et al.* 2000) obtained from the nearby study sites in the Northern Victoria Land. The  $\delta^{18}\text{O}$  ( $\delta\text{D}$ ) changed synchronously and showed clear seasonal variations, with the most enriched value occurring near the snow surface and at a depth of 90 cm. It can reasonably be assumed that the layers with  $\delta\text{D}$  and  $\delta^{18}\text{O}$  maxima and minima are summer and winter layers, respectively (Stenni *et al.* 2000; Kwak *et al.* 2015).

The snowpit was dated using the seasonal variations of isotopic compositions ( $\delta\text{D}$  and  $\delta^{18}\text{O}$ ). The 1.95-m deep snowpit contained snow deposited over a three-year period (2008–2010). The *d*-excess can be determined by the relative humidity of the ocean water in the source area of water vapor and sea surface temperature (Uemura *et al.* 2008). The mean *d*-excess was 8.22‰, with a maximum of 21.91‰ and a minimum of  $-0.11\text{‰}$  ( $n = 39$ ). Although the oscillation of the *d*-excess differed from those of  $\delta\text{D}$  and  $\delta^{18}\text{O}$ , the variation is relatively consistent, the lower variation in the seasonal cycle of *d*-excess values indicates dominant moisture transport from the neighboring stationary ocean source (Delmotte *et al.* 2000; Fujita and Abe 2006; Jouzel *et al.* 2007). In this region, Stenni *et al.* (2000) suggested the main influences originate from the Pacific Ocean and the Ross Sea.

**Chemical compositions of the snowpack.** – Sea-salt, derived from bubble-bursting and wind-blowing from wave crests in open-water and ice-covered areas, and oceanic biogenic activities have been considered as two major determinants of the chemical compositions of snow, firn cores, and ice cores in the coastal Antarctic (Delmas 1992; Wagenbach *et al.* 1998; Benassai *et al.* 2005).

High concentrations of sea-salt aerosols (e.g.  $\text{Na}^+$ ,  $\text{Mg}^{2+}$ ,  $\text{K}^+$ ,  $\text{Ca}^{2+}$ ,  $\text{Cl}^-$ , and  $\text{ssSO}_4^{2-}$ ) can



be seen in the winter layers of the snowpit, which are interpreted to be related to the thin layer of sea-salt enriched crystal that forms above sea ice and its movement with blowing snow (Rankin *et al.* 2005; Abram *et al.* 2007; Vega *et al.* 2018), which is greater than those transported from open sea during warm periods. Coupled with high cyclonic activities in the Ross Sea, mineral dust (partial of  $K^+$ ,  $Mg^{2+}$  and  $Ca^{2+}$ ) showed an enhancement in spring and summer in northern Victoria Land (Caiazza *et al.* 2017). This may be due to the input from local ice-free areas as well as long-range transport from South America (Kreutz *et al.* 1999).  $Na^+$  is a more reliable proxy for sea-spray aerosol due to the absence of extra sources, particularly in coastal regions, and to the steady concentration during transport and preservation without fractionation (Traversi *et al.* 2004).

The variation of the chemical composition of the snowpit is plotted in Figs 4 and 5. There were positive correlations ( $r > 0.85$ ) between  $Na^+$  and other ions ( $Cl^-$ ,  $SO_4^{2-}$ ,  $Ca^{2+}$ ,  $Mg^{2+}$ ,  $K^+$ ). The concentrations of  $Na^+$  and  $Cl^-$  showed similar profiles, with pronounced seasonal variations (Fig. 4). The winter-to-spring peak observed for  $Na^+$  and  $Cl^-$  is in agreement with previous studies conducted on the Antarctic ice sheet (Rankin *et al.* 2007; Stenni *et al.* 2000). A high concentration of sea salts can occur in winter due to intensive storms, which move the fragile sea-salt crystals formed above the sea-ice surface (Udisti *et al.* 1998; Rankin *et al.* 2000; Abram *et al.* 2007; Kavan *et al.* 2020). To investigate the seasonal changes of  $Na^+$  and  $Cl^-$  sources,  $Cl^-/Na^+$  ratios were computed (Fig. 4C). The ratios reached the sea-water ratio of 1.18 during the winter-to-spring period, while other periods showed a depletion of  $Cl^-$  concentrations compared to  $Na^+$  concentrations.

MSA and  $nssSO_4^{2-}$  are the oxidation products of dimethylsulfide (DMS) from marine algae and phytoplankton during the austral spring and summer (Udisti *et al.* 1998). Although  $nssSO_4^{2-}$  in polar ice cores can be derived from crustal erosion or volcanic emissions (Handler 1989; Delmas *et al.* 1992; Legrand and Mayewski 1997; Cole-Dai *et al.* 1999), emissions

from marine activity can be significant, especially at coastal sites (Dixon *et al.* 2004; Jonsell *et al.* 2005; Uemura *et al.* 2016). Although there can be differences in the transport pathways of MSA and  $\text{nssSO}_4^{2-}$  (Becagli *et al.* 2012), as well as differences in their rates of photochemical oxidation (Preunkert *et al.* 2008), the elevated MSA and  $\text{nssSO}_4^{2-}$  in the snowpit during the spring and early summer were related to the strong seasonality of DMS production ( $r = 0.60$ ). A similar seasonal pattern has been reported in previous studies (Udisti *et al.* 1998; Saltzman *et al.* 2006; Rhodes *et al.* 2012; Becagli *et al.* 2016). The MSA and  $\text{nssSO}_4^{2-}$  were lower in 2009. The MSA/ $\text{nssSO}_4^{2-}$  ratios (Fig. 5) showed a major peak in late summer to fall.

In this study, PCA was applied to the isotopic and chemical compositions of the snowpit to determine the factors that had the greatest influence on these compositions. In the present study, PCA was utilized to emphasize the dominant characteristics of the isotopic and chemical compositions of the snowpit at the same depth resolution. The inter-correlated variation, which represents the same atmospheric sources and common transport path (Knüsel *et al.* 2005; Kwak *et al.* 2015), is shown to assist the visual interpretation of the temporal signals by detecting the seasonal tendency. PCA was conducted using the variables,  $\delta^{18}\text{O}$ ,  $\text{Na}^+$ ,  $\text{K}^+$ ,  $\text{Mg}^{2+}$ ,  $\text{Ca}^{2+}$ , MSA,  $\text{Cl}^-$ ,  $\text{NO}_3^-$ , and  $\text{SO}_4^{2-}$ . The first principal component was loaded by most of ions except MSA and nitrate in all time periods (loading values are  $> 0.9$ ), which suggests that most of the major ions have a common and dominant source, for example, the nearby ocean (Moore *et al.* 2005; Kwak *et al.* 2015) (Table 2). As shown in Table 2, the strong positive correlations ( $r$ ) were observed among the ions ( $\text{Na}^+$ ,  $\text{K}^+$ ,  $\text{Ca}^{2+}$ ,  $\text{Mg}^{2+}$  and  $\text{Cl}^-$ ;  $r > \sim 0.85$ ). The second principal component had high loadings of  $\delta^{18}\text{O}$ , MSA, and  $\text{NO}_3^-$ , which indicates the seasonal nature of these variables. PCA classified the variables into species representing input of sea-salt aerosol (PC 1) and species suggesting potential seasonal markers (PC 2). This result is consistent with what Nyamgerel *et al.* (2020) reported in the

Styx firn core.

### Summary and implication of this work

This study focused on the water isotopic and chemical composition of snowpit samples and four surface snow samples obtained from a coastal site near to the JBS in northern Victoria Land, East Antarctica. The isotopic and chemical compositions of the surface snow represent distinct values, mainly depending on the distance to the coast, and indicate that the source of the snow is oceanic. The snowpit shows a typical variation of isotopic compositions, with the slope of the  $\delta D$ - $\delta^{18}O$  diagram for the snowpack being  $8.2 (\pm 0.2)$ . This also indicates that the vapor source is from the nearby ocean by evaporation. Based on the seasonal layers with  $\delta D$  and  $\delta^{18}O$  maxima and minima, the snowpit was determined to contain snow deposited over a three-year period (2008–2010). Although the record is short, it can be seen that the major contribution is from an oceanic source based on the positive correlations ( $r > 0.85$ ) between sea-salt ions. Moreover, the MSA and  $nssSO_4^{2-}$  in the snowpit elevated values fairly with the isotopic peaks. Via PCA, the variables were classified into species representing input of sea-salt aerosol (PC 1) and species suggesting potential seasonal markers (PC 2). This study will be supportive for further investigations in this region.

**Acknowledgements.** This work was financially supported by a research grant (PE21100) from the Korea Polar Research Institute. Remarks from two anonymous reviewers improved the quality of the paper.

### References

Abram N.J., Mulvaney R., Wolff E.W. and Mudelsee M. 2007. Ice core records as sea ice proxies: an evaluation from the Weddell Sea region of Antarctica. *Journal of Geophysical Research-Atmospheres* 112: D15101.

- Arndt S. and Paul S. 2018. Variability of winter snow properties on different spatial scales in the Weddell Sea. *Journal of Geophysical Research-Oceans* 123: 8862– 8876.
- Ayling B.F. and MCGowan H.A. 2006. Niveo-eolian sediment deposits in coastal South Victoria Land, Antarctica: Indicators of regional variability in weather and climate. *Arctic, Antarctic, and Alpine Research* 38: 313–324.
- Becagli S., Scarchilli C., Traversi R., Dayan U., Severi M., Frosini D., Vitale V., Mazzola M., Lupi A., Nava S. and Udisti R. 2012. Study of present-day sources and transport processes affecting oxidized sulphur compounds in atmospheric aerosols at Dome C (Antarctica) from year-round sampling campaigns. *Atmospheric Environment* 52: 98–108.
- Becagli S., Lazzara L., Marchese C., Dayan U., Ascanius S.E., Cacciani M., Caiazzo L., Di Biagio C., Di Iorio T., Di Sarra A., Eriksen P., Fani F., Giardi F., Meloni D., Muscari G., Pace G., Severi M., Traversi R. and Udisti R. 2016. Relationships linking primary production, sea ice melting, and biogenic aerosol in the Arctic. *Atmospheric Environment* 136: 1–15.
- Benassai, S., Becagli, S., Gragnani, R., Magand, O., Proposito, M., Fattori, I. and Udisti R. 2005. Sea-spray deposition in Antarctic coastal and plateau areas from ITASE traverses. *Annals of Glaciology* 41: 32–40.
- Caiazzo L., Baccolo G., Barbante C., Becagli S., Berto M., Ciardini V., Crotti V., Delmonte B., Dreossi G., Frezzotti M., Gabrieli J., Giardi F., Han Y., Hong S.B., Hur S.D., Hwang H., Kang J.H., Narcisi B., Proposito M., Scarchilli C., Selmo E., Severi M., Spolaor A., Stenni B., Traversi R. and Udisti R. 2017. Prominent features in isotopic, chemical and dust stratigraphies from coastal East Antarctic ice sheet (Eastern Wilkes Land). *Chemosphere* 176: 273–287.
- Casado M., Landais A., Picard G., Münch T., Laepple T., Stenni B., Dreossi, G., Ekaykin A., Arnaud L., Genthon C., Touzeau A., Masson-Delmotte V. and Jouzel J. 2018. Archival processes of the water stable isotope signal in East Antarctic ice cores. *The Cryosphere* 12: 1745–1766.
- Cole-Dai J., Mosley-Thompson E. and Qin D. 1999. Evidence of the 1991 Pinatubo volcanic eruption in South Polar snow. *Chinese Science Bulletin* 44:756–760.
- Dansgaard W. 1964. Stable isotopes in precipitation. *Tellus* 16: 436–468.
- Delmas R.J., Kirchner S., Palais J.M. and Petit J.R. 1992. 1000 years of explosive volcanism recorded at the South Pole. *Tellus B* 44: 335–350.

- Delmotte M., Masson V., Jouzel J. and Morgan V.I. 2000. A seasonal deuterium excess signal at Law Dome, coastal eastern Antarctica: A Southern Ocean signature. *Journal of Geophysical Research-Atmospheres* 105: 7187–7197.
- Dixon D., Mayewski P., Kaspari S., Sneed S. and Handley M. 2004. A 200 year sub-annual record of sulfate in West Antarctica, from 16 ice cores. *Annals of Glaciology* 39: 545–556.
- Du Z., Xiao C., Zhang Q., Handley M.J., Paul A., Mayewski A. and Li C. 2019. Relationship between the 2014–2015 Holuhraun eruption and the iron record in the East GRIP snow pit. *Arctic, Antarctic, and Alpine Research* 51: 290–298.
- Fujita K. and Abe O. 2006. Stable isotopes in daily precipitation at Dome Fuji, East Antarctica, *Geophysical Research Letters* 33: L18503.
- Goursaud S., Masson-Delmotte V., Favier V., Preunkert S., Legrand M., Minster, B. and Werner M. 2019. Challenges associated with the climatic interpretation of water stable isotope records from a highly resolved firn core from Adélie Land, coastal Antarctica. *The Cryosphere* 13: 1297–1324.
- Ham J., Hur S., Lee W., Han Y., Jung H. and Lee, J. 2019. Isotopic variations of meltwater from ice by isotopic exchange between liquid water and ice. *Journal of Glaciology* 65: 1035–1043.
- Handler P. 1989. The effect of volcanic aerosols on global climate. *Journal Volcanology and Geothermal Research* 37: 233–249.
- Jonsell U., Hansson M.E., Morth C-M. and Torssander P. 2005. Sulfur isotopic signals in two shallow ice cores from Dronning Maud Land, Antarctica. *Tellus B: Chemical and Physical Meteorology* 57: 341–350.
- Jouzel J., Masson-Delmotte V., Cattani O., Dreyfus G., Falourd S., Hoffmann G., Minster B., Nouet J., Barnola J.M., Chappellaz J., Fischer H., Gallet J.C., Johnsen S., Leuenberger M., Loulergue L., Luethi D., Oerter H., Parrenin F., Raisbeck G., Raynaud D., Schilt A., Schwander J., Selmo E., Souchez R., Spahni R., Stauffer B., Steffensen J.P., Stenni B., Stocker T.F., Tison J.L., Werner M. and Wolff E.W. 2007. Orbital and millennial Antarctic climate variability over the past 800000 years. *Science* 317: 793–796.
- Jouzel J. and Masson-Delmotte V. 2010. Paleoclimates: what do we learn from deep ice cores? *WIREs Climate Change* 1: 654–669.

- Kavan J., Nyvlt D., Laska K., Engel Z. and Knazkova M. 2020. High-latitude dust deposition in snow on the glaciers of James Ross Island, Antarctica. *Earth Surface Processes and Landforms* 45: 1569–1578.
- Knusel S., Brutsch S., Henderson K.A., Palmer A.S. and Schwikowski M. 2005. ENSO signals of the twentieth century in an ice core from Nevado Illimani, Bolivia. *Journal of Geophysical Research* 110: D01102.
- Ko K.S., Lee J. and Lee K.K. 2010. Multivariate statistical analysis for groundwater mixing ratios around underground storage caverns in Korea. *Carbonates Evaporites* 25: 35–42.
- Klein N.F., Abram N.J., Curran M.A.J., Goosse H., Goursaud S., Masson-Delmotte V., Moy A., Neukom R., Orsi A., Sjolte J., Steiger N., Stenni B. and Werner M. 2019. Assessing the robustness of Antarctic temperature reconstructions over the past 2 millennia using pseudoproxy and data assimilation experiments. *Climate of the Past* 15: 661–684.
- Kreutz K.J. and Mayewski P.A. 1999. Spatial variability of Antarctic surfaces snow glaciochemistry: Implications for paleoatmospheric circulation reconstructions. *Antarctic Science* 11: 105–118.
- Kuramoto, T., Goto-Azuma K., Hirabayashi, M., Miyake, T., Motoyama, H., Dahl-Jensen, D. and Steffensen J. 2011. Seasonal variations of snowchemistry at NEEM, Greenland. *Annals of Glaciology* 52: 193–200.
- Kwak H., Kang J-H., Hong S-B., Lee J., Chang C., Hur S-D. and Hong S. 2015. A Study on High-Resolution Seasonal Variations of Major Ionic Species in Recent Snow Near the Antarctic Jang Bogo Station. *Ocean and Polar Research* 37: 127–140.
- Lee J., Ko K., Kim J. and Chang H. 2008. Multivariate statistical analysis of underground gas storage caverns on groundwater chemistry in Korea. *Hydrological Processes* 22: 3410–3417.
- Lee J., Feng X., Posmentier E.S., Faiia A.M. and Taylor S. 2009. Stable isotopic exchange rate constant between snow and liquid water. *Chemical Geology* 260: 57–62.
- Lee J., Feng X., Faiia A.M., Posmentier E.S., Kirchner J.W., Osterhuber R. and Taylor S. 2010. Isotopic evolution of a seasonal snowcover and its melt by isotopic exchange between liquid water and ice. *Chemical Geology* 270: 126–134.
- Lee J. 2014. A numerical study of isotopic evolution of a seasonal snowpack and its meltwater by total rates. *Geosciences Journal* 18, 503–510.
- Lee J., Hur S.D., Lim H.S. and Jung H.J. 2020. Isotopic characteristics of snow and its

- meltwater over the Barton Peninsula, Antarctica. *Cold Regions Science and Technology* 173: 102997.
- Legrand M. and Mayewski P. 1997. Glaciochemistry of polar ice cores: A review. *Review of Geophysics* 35: 219–243.
- Ma T., Li L., Li Y., Aa C., Ma H., Jiang S. and Shi G. 2020. Stable isotopic composition in snowpack along the traverse from a coastal location to Dome A (East Antarctica): Results from observations and numerical modeling. *Polar Science* 24: 100510.
- Markle B.R., Bertler N.A.N., Sinclair K.E. and Sneed S.B. 2012. Synoptic variability in the Ross Sea region, Antarctica, as seen from back-trajectory modeling and ice core analysis. *Journal of Geophysical Research* 117: 1–17.
- Masoon-Delmotte V., Hou S., Ekaykin A., Jouzel J., Aristarain A., Bernardo R.T., Bromwich D., Attani O., Delmotte M., Falourd S., Frezzotti M., Gallee H., Genoni L., Isaksson E., Landais A., Helsen M.M., Hoffmann G., Lopez J., Morgan V., Motoyama H., Noone D., Oerter H., Petit J.R., Royer A., Uemura R., Schmidt G.A., Schlosser E., Simoes J.C., Steig E.J., Stenni B., Stievenard M., Van Den Broeke M.R., Van De Wal R.S.W., Van De Berg W.J., Vimeux F. and White J.W.C. 2008. A review of Antarctic surface snow isotopic composition: Observations, atmospheric circulation, and isotopic modeling. *Journal of Climate* 21: 3359–3387.
- Moore J.C., Grinsted A., Kekonen T. and Pohjola V. 2005. Separation of melting and environmental signals in an ice core with seasonal melt. *Geophysical Research Letters* 32: L10501.
- Nyamgerel Y., Han Y., Kim S., Hong S., Lee J. and Hur S. 2020. Chronological characteristics for snow accumulation on Styx Glacier in northern Victoria Land, Antarctica. *Journal of Glaciology* 66: 916–926.
- Nyamgerel Y., Hong S., Han Y., Kim S., Lee J. and Hur S. 2021. Snow-pit record from a coastal Antarctic site and its preservation of meteorological features. *Earth Interactions* 25: 108–118.
- Park Y., Yoo H.J., Lee W.S., Lee J., Kim Y., Lee S-H., Shin D. and Park H. 2014. Deployment and Performance of a Broadband Seismic Network near the New Korean Jang Bogo Research Station, Terra Nova Bay, East Antarctica. *Seismological Research Letters* 85: 1341–1347.
- Preukert S., Jourdain B., Legrand M., Udisti R., Becagli S. and Cerri O. 2008. Seasonality of sulfur species (dimethylsulfide, sulfate, and methanesulfonate) in Antarctica: inland versus coastal regions. *Journal of Geophysical Research* 113: D15302.



- Rankin A.M., Auld V. and Wolff E.W. 2000. Frost flowers as a source of fractionated sea salt aerosol in the polar regions. *Geophysical Research Letters* 27: 3469–3472.
- Rhodes, R.H., Bertler, N.A.N., Baker, J.A., Steen-Larsen, H.C., Sneed, S.B., Morgenstern, U. and Johnsen, S.J. 2012. Little Ice Age climate and oceanic conditions of the Ross Sea, Antarctica from a coastal ice core record. *Climate of the Past* 8: 1223–1238.
- Saltzman E.S., Dioumaeva I. and Finley B.D. 2006. Glacial/interglacial variations in methanesulfonate (MSA) in the Siple Dome ice core, West Antarctica. *Geophysical Research Letters* 33: L11811.
- Servettaz A.P.M., Orsi A.J., Curran M.A.J., Moy A.D., Landais, A., Agosta C., Winton V.H.L., Touzeau A., McConnell J.R., Werner M. and Baroni M. 2020. Snowfall and water stable isotope variability in East Antarctica controlled by warm synoptic events. *Journal of Geophysical Research-Atmosphere* 125: e2020JD032863.
- Severi M., Becagli S., Caiazzo L., Ciardini V., Colizza E., Giardi F., Mezgec K., Scarchilli C., Stenni B., Thomas E.R., Traversi R. and Udisti R. 2017. Sea salt sodium record from Talos Dome (East Antarctica) as a potential proxy of the Antarctic past sea ice extent. *Chemosphere* 177: 266–274.
- Sinclair K.E., Bertler N.A.N. and Trompeter W.J. 2010. Synoptic controls on precipitation pathways and snow delivery to high-accumulation ice core sites in the Ross Sea region, Antarctica. *Journal of Geophysical Research* 115: D22112.
- Steen-Larsen H.C., Masson-Delmotte V., Hirabayashi M., Winkler R., Satow K., Prie F., Bayou N., Brun E., Cuffey K.M., Dahl-Jensen D., Dumont, M., Guillevic M., Kipfstuhl S., Landais A., Popp T., Risi C., Steffen, K., Stenni B. and Sveinbjornsdottir A.E. 2014. What controls the isotopic composition of Greenland surface snow?. *Climate of the Past* 10: 377–392.
- Stenni B., Caprioli R., Cimino L., Cremisini C., Flora O., Gagnani R. and Torcini S. 1999. 200 Years of Isotope and Chemical Records in a Firn Core from Hercules N ev e, Northern Victoria Land, Antarctica. *Annals of Glaciology* 29: 106–112.
- Stenni B., Serra F., Frezzotti M., Maggi V., Traversi R., Becagli S. and Udisti R. 2000. Snow accumulation rates in northern Victoria Land, Antarctica, by firn-core analysis. *Journal of Glaciology* 46: 541–552.
- Stenni B., Curran M.A.J., Abram N.J., Orsi A., Goursaud S., Masson-Delmotte V., Neukom R., Goosse H., Divine D., Van Ommen T., Steig E.J., Dixon D.A., Thomas E.R., Bertler N.A.N., Isaksson E., Ekaykin A., Werner M. and Frezzotti M. 2017. Antarctic



- climate variability on regional and continental scales over the last 2000 years. *Climate of the Past* 13: 1609–1634.
- Traversi R., Becagli S., Castellano E., Largiuni O., Migliori A., Severi M., Frezzotti M. and Udisti R. 2004. Spatial and temporal distribution of environmental markers from coastal to plateau areas in Antarctica by firn core chemical analysis. *International Journal of Environmental Analytical Chemistry* 84: 457–470.
- Tuohy A., Bertler N., Neff P., Edwards R., Emanuelsson D., Beers T. and Mayewski P. 2015. Transport and deposition of heavy metals in the Ross Sea Region, Antarctica. *Journal of Geophysical Research-Atmosphere* 120: 10,996–11,011.
- Udisti R. 1996. Multiparametric approach for chemical dating of snow layers from Antarctica. *International Journal of Environmental Analytical Chemistry* 63: 225–244.
- Udisti R., Traversi R., Becagli G. and Picaardi G. 1998. Spatial distribution and seasonal pattern of biogenic sulphur compounds in snow from northern Victoria Land, Antarctica. *Annals of Glaciology* 27: 535–542.
- Udisti R., Barbante C., Castellano E., Vermigli S., Traversi R., Capodaglio G. and Picaardi G. 1999. Chemical characterisation of a volcanic event (about AD 1500) at Styx Glacier plateau, northern Victoria Land, Antarctica. *Annals of Glaciology* 29: 113–120.
- Uemura R., Masaka K., Fukui K., Iizuka Y., Hirabayashi M. and Motoyama H. 2016. Sulfur isotopic composition of surface snow along a latitudinal transect in East Antarctica. *Geophysical Research Letters* 43: 5878–5885.
- Vega C.P., Isaksson E., Schlosser E., Divine D., Martma T., Mulvaney R., Eichler A. and Schwikowski-Gigar M. 2018. Variability of sea salts in ice and firn cores from fimbria ice shelf, Dronning Maud Land, Antarctica. *The Cryosphere* 12: 1681–1697.
- Wagenbach D., Legrand M., Fischer H., Pichlmayer F. and Wolff E.W. 1998. Atmospheric near-surface nitrate at coastal Antarctic sites. *Journal of Geophysical Research-Atmospheres* 103: 11007–11020.
- Wang J., Kim J., Choi, W., Mun, D., Kang, J., Kwon, H., Kim, J. And Han K. 2017. Effects of wind fences on the wind environment around Jang Bogo Antarctic Research Station. *Advances in Atmospheric Sciences* 34: 1404–1414.

Received 7 March 2021

Accepted 9 July 2021

Table 1. The isotopic and chemical compositions of four snow samples (JBG-01, JBG-01, JBG-03, JBG-04) and snowpit.

	JBG-01	JBG-02	JBG-03	JBG-04	Snowpit mean	Snowpit SD*
Location	S74° 36.665' E164° 13.536'	S74° 37.097' E164° 12.239'	S74° 37.249' E164° 11.644'	S74° 37.489' E164° 12.894'	S74° 25.344' E164° 10.429'	
MSA	47.88	522.62	494.68	504.28	36.59	32.54
Cl <sup>-</sup>	759.21	15,329.19	10,997.50	20,394.78	493.51	546.08
SO <sub>4</sub> <sup>2-</sup>	212.73	2614.34	2085.81	3166.07	205.70	116.18
NO <sub>3</sub> <sup>-</sup>	189.08	1582.84	1469.41	1587.28	64.24	78.81
Na <sup>+</sup>	412.45	8674.51	6406.89	11,635.68	298.32	312.94
K <sup>+</sup>	70.43	582.13	565.36	376.85	22.32	18.95
Mg <sup>2+</sup>	175.86	2160.94	1916.33	2495.20	56.05	68.89
Ca <sup>2+</sup>	74.94	3262.69	3078.66	3248.20	51.64	71.95
δ <sup>18</sup> O	-13.88	-14.86	-18.15	-16.77	-24.34	4.84
δD	-99.48	-117.88	-146.55	-130.79	-186.50	39.82
d-excess	11.57	0.98	-1.36	3.35	8.22	5.16

\* SD - standard deviation.

Table 2. Correlation matrix for the principal component analysis. The correlation coefficient values greater than 0.5 were highlighted in bold ( $n=39$ )

	$\delta^{18}\text{O}$	MSA	$\text{Cl}^-$	$\text{SO}_4^{2-}$	$\text{NO}_3^-$	$\text{Na}^+$	$\text{K}^+$	$\text{Mg}^{2+}$	$\text{Ca}^{2+}$
$\delta^{18}\text{O}$	1.00								
MSA	0.10	1.00							
$\text{Cl}^-$	<b>-0.61</b>	0.08	1.00						
$\text{SO}_4^{2-}$	-0.31	0.45	<b>0.80</b>	1.00					
$\text{NO}_3^-$	-0.18	0.28	<b>0.57</b>	<b>0.83</b>	1.00				
$\text{Na}^+$	<b>-0.57</b>	0.10	1.00	<b>0.83</b>	<b>0.59</b>	1.00			
$\text{K}^+$	<b>-0.54</b>	0.10	<b>0.99</b>	<b>0.84</b>	<b>0.61</b>	<b>0.99</b>	1.00		
$\text{Mg}^{2+}$	<b>-0.61</b>	0.07	1.00	<b>0.80</b>	<b>0.55</b>	<b>0.99</b>	<b>0.99</b>	1.00	
$\text{Ca}^{2+}$	-0.38	0.14	<b>0.87</b>	<b>0.91</b>	<b>0.76</b>	<b>0.89</b>	<b>0.91</b>	<b>0.88</b>	1.00

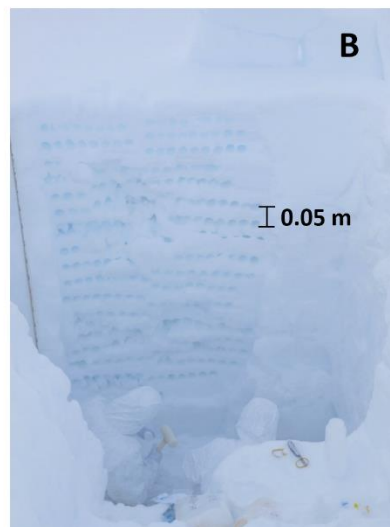
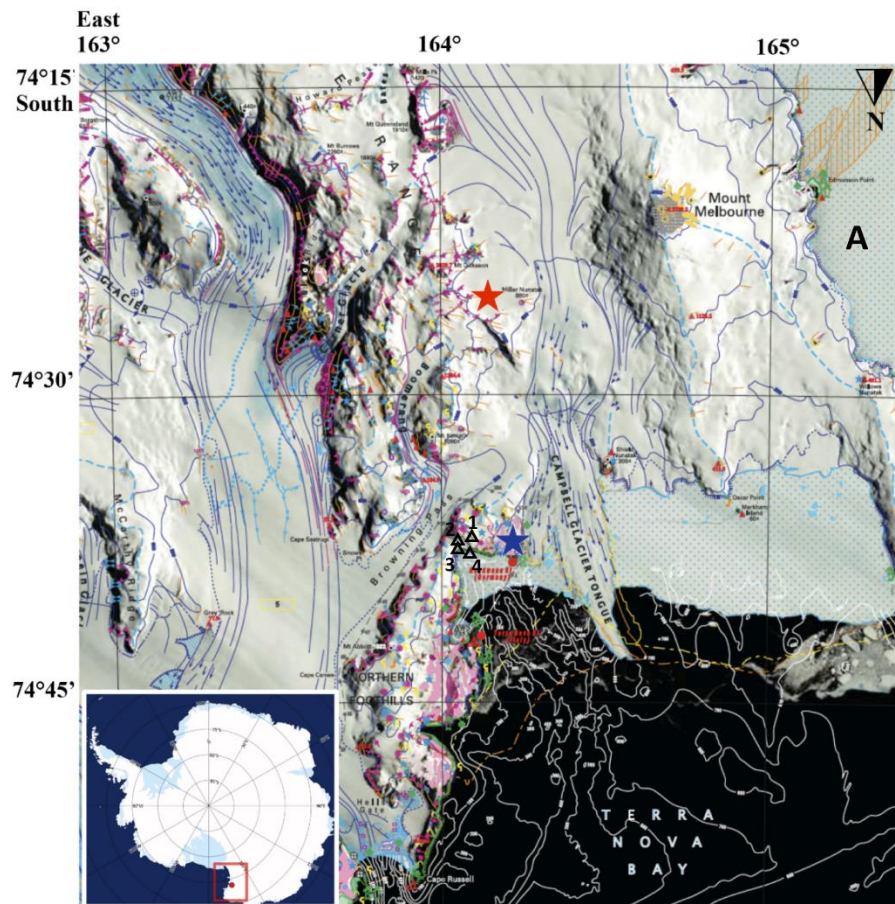


Fig. 1. (A) Location of the snowpit (red star) near the Korean Jang Bogo Station (blue star) in Terra Nova Bay, East Antarctica. Surface snow samples (numbers) are located just near by the station. The surface snow samples were collected before the construction of JBS. The locations of samples were indicated in Table 1. (B) photo of snowpit.

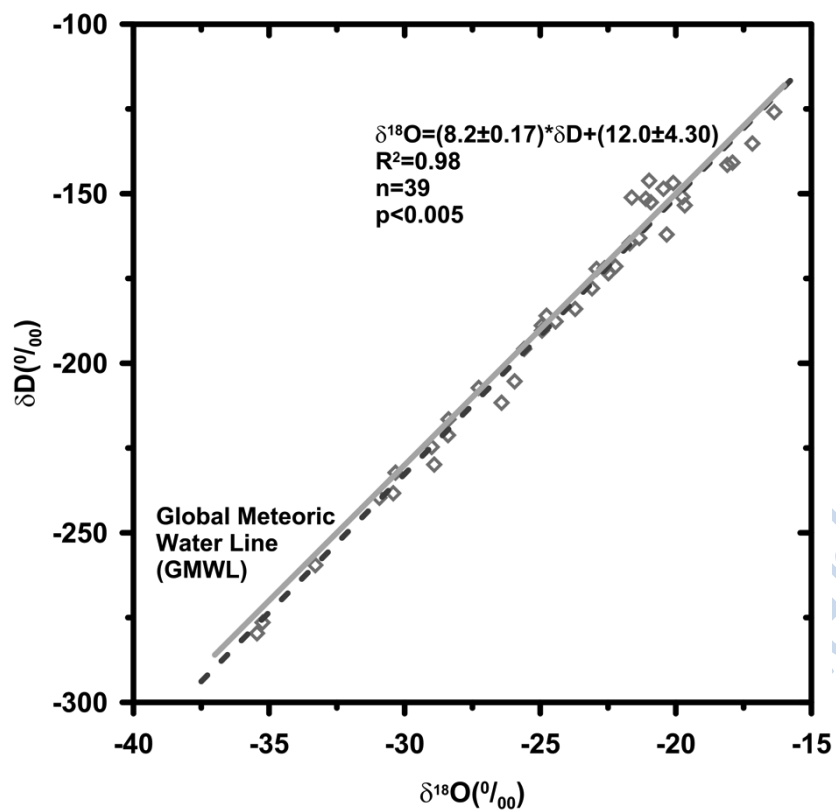


Fig. 2. The linear regression line between  $\delta D$  and  $\delta^{18}O$ . The regression line is similar to that of the GMWL (grey line).

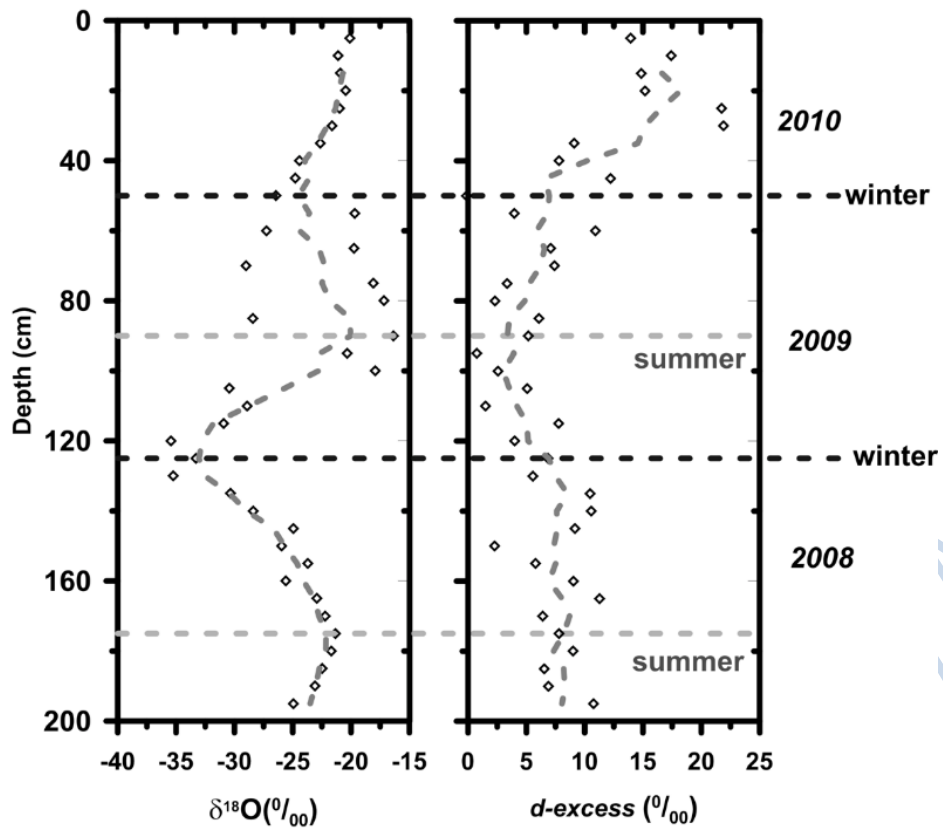


Fig. 3. Vertical profiles of stable water isotopes ( $\delta^{18}\text{O}$  in the left and deuterium excess in the right, respectively). Summer and winter in the snowpit were defined from the maximum and minimum values of the stable water isotopes, respectively.

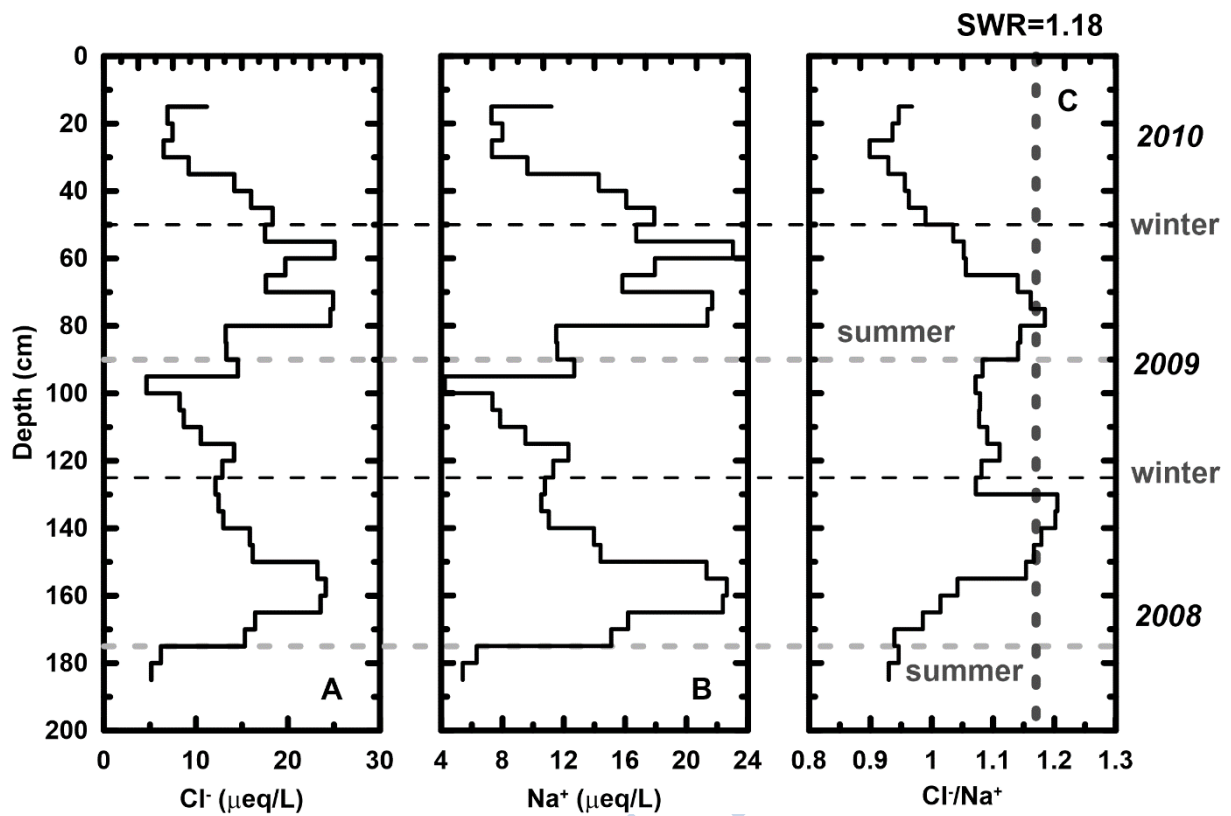


Fig. 4. Vertical profiles of  $\text{Cl}^-$  (A),  $\text{Na}^+$  (B) and the  $\text{Cl}^-/\text{Na}^+$  ratio (C). The dashed line represents the  $\text{Cl}^-/\text{Na}^+$  ratio in the Sea Water Ratio (SWR, 1.18).

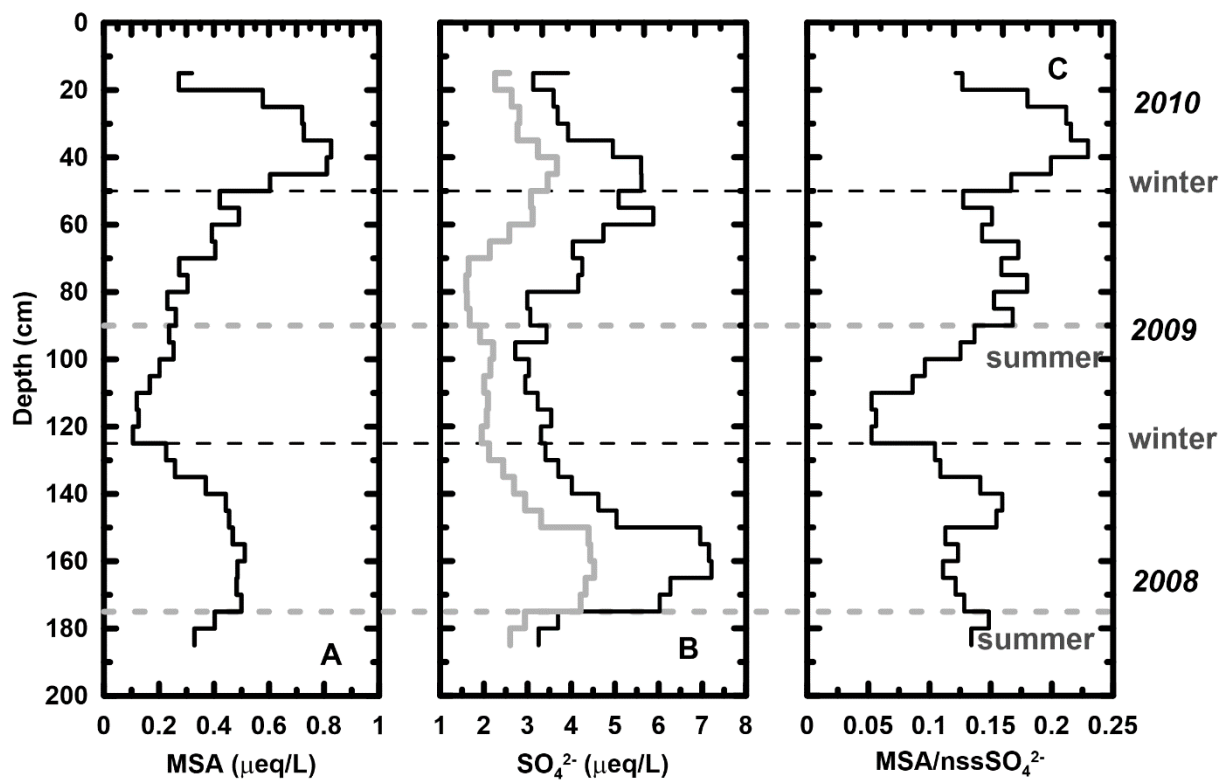


Fig. 5. Vertical profiles of methanesulfonate (MSA) (A), sulfate (B), and MSA/nssSO<sub>4</sub><sup>2-</sup> ratio (C). The gray line in the middle indicates non-sea-salt (nssSO<sub>4</sub><sup>2-</sup>).